Density-dependent effective nucleon-nucleon interaction from chiral three-nucleon forces*

J. W. Holt, N. Kaiser, and W. Weise

Physik Department, Technische Universität München, D-85747 Garching, Germany

Abstract

We derive density-dependent corrections to the in-medium nucleon-nucleon interaction from the leading-order chiral three-nucleon force. To this order there are six distinct one-loop diagrams contributing to the in-medium nucleon-nucleon scattering T-matrix. Analytic expressions are presented for each of these in both isospin-symmetric nuclear matter as well as nuclear matter with a small isospin asymmetry. The results are combined with the low-momentum nucleon-nucleon potential $V_{\rm low-k}$ to obtain an effective density-dependent interaction suitable for nuclear structure calculations. The in-medium interaction is decomposed into partial waves up to orbital angular momentum $L = 2$. Our results should be particularly useful in calculations where an exact treatment of the chiral three-nucleon force would otherwise be computationally prohibitive.

* Work supported in part by BMBF, GSI and by the DFG cluster of excellence: Origin and Structure of the Universe.

I. INTRODUCTION

Three-body forces play an essential role in describing the detailed properties of nuclear many-body systems. Compelling evidence for this arises from the inability of non-relativistic nucleon-nucleon (NN) interactions alone to accurately reproduce (i) the saturation properties of nuclear matter, (ii) the binding energies and spectra of light nuclei, and (iii) nucleon-deuteron scattering differential cross sections at intermediate energies. These systems are simple enough that the uncertainties associated with the solution of the corresponding many-body equation are well controlled, and therefore deviations from experimental data are interpreted as deficiencies in the underlying nuclear force model.

In the case of nuclear matter, a variety of methods such as the Brueckner-Bethe-Goldstone hole-line expansion [1, 2], variational methods [3, 4], and the summation of particle-particle hole-hole ring diagrams [5, 6] all produce similar results for the energy per particle as a function of the density. However, these calculations result in a series of saturation points that lie at either too high a density or too low a binding energy compared to the empirical values of $\rho_0 = 0.16$ fm^{-3} and $E/A = -16$ MeV. Numerous solutions to this problem have been proposed, such as including relativistic effects [7, 8], three-nucleon forces [9, 10], or medium-modified meson masses [11, 12]. The analogous problem in light nuclei is that calculated binding energies come out $\sim 10 - 15\%$ smaller than experimental values when two-body interactions alone are used [13, 14, 15]. By including various models of the three-nucleon force, several groups have shown that not only the nuclear binding energy problem can be remedied but the low-lying spectra of light nuclei can also be greatly improved [15, 16, 17]. Finally, the differential cross section for elastic nucleon-deuteron scattering at intermediate energies ($E_N^{\rm lab} = 100 - 300$ MeV) exhibits a minimum at backward angles that is larger by nearly 30% compared to Faddeev calculations using NN interactions alone [18, 19]. This discrepancy is well accounted for when effects from three-body forces [20] or (equivalently) explicit Δ isobar degrees of freedom [18, 21] are included.

The preceding examples illustrate the limitations in obtaining precise agreement with various nuclear observables when using only two-body interactions that are fit to free-space NN scattering data. Although there has been much effort devoted to the construction of realistic models of the three-nucleon force, it is technically very challenging to include them in large-scale calculations of medium and heavy nuclei. An alternative and simpler approach is to employ instead density-dependent two-body interactions that reflect the underlying three-nucleon forces. Therefore, the purpose of the present work is to construct a density-dependent in-medium NN interaction that is generated at one-loop order by the genuine three-nucleon force. We

have found in ref. [22] that such density-dependent corrections to the NN interaction strongly suppress the ^{14}C ground state to ^{14}N ground state Gamow-Teller transition and in this way helps to explain the anomalously long lifetime of ^{14}C. We work within the framework of chiral effective field theory and take into account the leading-order three-nucleon forces arising in that systematic approach. We consider first the density-dependent terms in isospin symmetric nuclear matter and then continue with the leading (linear) effects due to an isospin asymmetry, which are likely to be relevant for heavy nuclei. The paper is organized as follows. In section II we briefly describe the chiral effective field theory approach to nuclear interactions, together with the explicit form of the leading-order three-nucleon force. In section III we evaluate the one-loop corrections to NN scattering in the nuclear medium generated by this chiral three-nucleon force. In section IV we present numerical results for the in-medium NN interaction in partial waves up to orbital angular momentum $L = 2$. The paper ends with a summary and conclusions.

II. NUCLEAR INTERACTIONS FROM EFFECTIVE FIELD THEORY

A. Chiral effective interactions

Chiral effective field theory provides a useful tool for describing a wide range of low-energy hadronic phenomena within a single consistent framework. The theory exploits the natural separation of energy scales that results from the spontaneous (and explicit) breaking of chiral symmetry in QCD, which gives rise to light pseudoscalar Goldstone bosons (the pion triplet in the two flavor case). These, together with nucleons, comprise the low energy degrees of freedom of the theory. Long-range effects from one- and two-pion exchange between nucleons are treated explicitly, while the short-distance dynamics due to heavy mesons and baryon resonances (with the possible exception of the Δ isobar) are integrated out and their effects are encoded in nucleon contact terms. Presently the computation of the chiral NN potential has been carried out to next-to-next-to-next-to-leading order (N^{3}LO) in the small momentum expansion [23, 24, 25, 26]. At this order it is possible to achieve an agreement with empirical NN scattering phase shifts that is comparable to previous high-precision NN potentials [27, 28, 29]. By adjusting the 29 parameters (mostly low-energy constants) that occur at this order, the 1999 database for np and pp elastic scattering up to $E_{\rm lab} = 290$ MeV can be fit with a χ^2/dof of 1.1 for np scattering and 1.5 for pp scattering. Furthermore, the experimental deuteron binding energy, charge radius, and electric quadrupole moment are very well reproduced by the chiral

N^{3}LO potential [26]. When applied to two- and few-nucleon problems, these chiral potentials are regulated by exponential functions [23, 30] with cutoffs ranging from 500 to 700 MeV in order to eliminate high-momentum components. In addition, in-medium chiral perturbation theory which emphasizes the role of explicit two-pion-exchange dynamics in nuclear matter has been developed in ref. [31].

Three-nucleon forces arise first at third-order in the chiral power counting [32]. Three components of different range, shown by diagrams (a),(b), and (c) in Fig. 1, occur at this order and have the following analytic structure

$$V_{3N}^{(2\pi)} = \sum_{i\neq j\neq k} \frac{g_A^2}{8f_\pi^4} \frac{\vec{\sigma}_i\cdot\vec{q}_i\,\vec{\sigma}_j\cdot\vec{q}_j}{(\vec{q}_i^{\,2}+m_\pi^2)(\vec{q}_j^{\,2}+m_\pi^2)} F_{ijk}^{\alpha\beta}\tau_i^\alpha\tau_j^\beta, \tag{1}$$

$$V_{3N}^{(1\pi)} = -\sum_{i\neq j\neq k} \frac{g_A c_D}{8f_\pi^4\Lambda_\chi} \frac{\vec{\sigma}_j\cdot\vec{q}_j}{\vec{q}_j^{\,2}+m_\pi^2} \vec{\sigma}_i\cdot\vec{q}_j\,\vec{\tau}_i\cdot\vec{\tau}_j, \tag{2}$$

$$V_{3N}^{(\mathrm{ct})} = \sum_{i\neq j\neq k} \frac{c_E}{2f_\pi^4\Lambda_\chi} \vec{\tau}_i\cdot\vec{\tau}_j, \tag{3}$$

where $\vec{q}_i = \vec{p}_i\,' - \vec{p}_i$ is the difference between the final and initial momentum of nucleon i and

$$F_{ijk}^{\alpha\beta} = \delta^{\alpha\beta}\left(-4c_1m_\pi^2 + 2c_3\vec{q}_i\cdot\vec{q}_j\right) + c_4\epsilon^{\alpha\beta\gamma}\tau_k^\gamma\vec{\sigma}_k\cdot(\vec{q}_i\times\vec{q}_j)\,. \tag{4}$$

Together with $g_A = 1.29$ and $f_\pi = 92.4$ MeV, the parameters of $V_{3N}^{(2\pi)}$, namely $c_1 = -0.81\,\mathrm{GeV}^{-1}$, $c_3 = -3.2\,\mathrm{GeV}^{-1}$, and $c_4 = 5.4\,\mathrm{GeV}^{-1}$, are well determined from fits to low-energy NN phase shifts and mixing angles [23]. Restricting the two large coefficients $c_{3,4}$ to their dominant $\Delta(1232)$-resonance contributions, one reproduces the celebrated three-nucleon force of Fujita and Miyazawa [33]. The medium-range ($V_{3N}^{(1\pi)}$) and short-range ($V_{3N}^{(\mathrm{ct})}$) components are proportional to two new low-energy constants c_D and c_E, respectively. These constants can be fixed by fitting properties of few-nucleon systems, such as the triton binding energy together with the nd doublet scattering length [34], the ^{4}He binding energy [35], or binding energies and spectra of light nuclei [17]. At next order (in the chiral expansion) there are many additional one-loop diagrams contributing to the chiral three-nucleon force [32], but no new low-energy constants appear. The explicit construction of all these terms is currently in progress.

B. Low-momentum nuclear interaction

Recently there has been much interest in understanding the scale-dependence of NN interactions from the point of view of the renormalization group [36, 37]. In most applications of

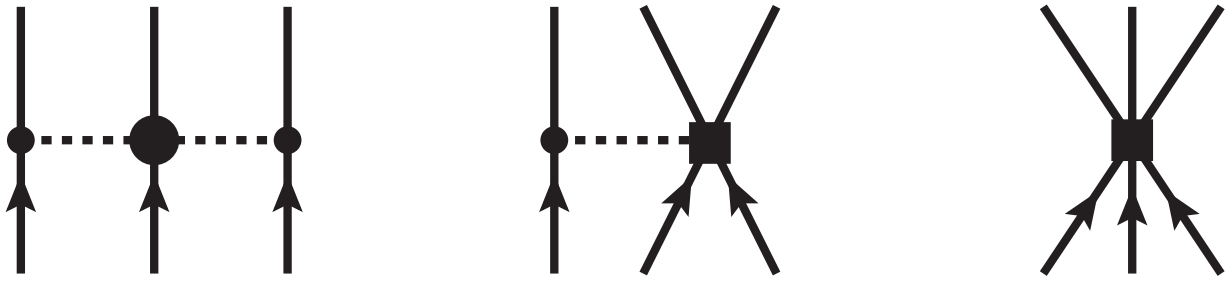

FIG. 1: The leading-order contributions to the chiral three-nucleon force: (a) the long-range 2π-exchange force $V_{3N}^{(2\pi)}$, (b) the medium-range 1π-exchange force $V_{3N}^{(1\pi)}$, and (c) the short-range contact interaction $V_{3N}^{(\mathrm{ct})}$.

chiral effective field theory to few-nucleon systems, exponential regulator functions with cutoffs between 500 and 700 MeV are used to eliminate the high-momentum components from the NN interaction. In fact, all realistic NN potentials are fit to *pp* and *pn* scattering data below a laboratory energy of 350 MeV and therefore are constrained experimentally only up to a momentum of $p_{\max} \simeq 400$ MeV $= 2.1$ fm^{-1}. Bogner and collaborators [36, 37] have shown how to evolve any bare NN interaction down to a low-momentum scale via renormalization group techniques. Such low-momentum interactions $V_{\mathrm{low-k}}$ are phase-shift equivalent to the underlying bare interaction at energies below the specified cutoff scale $\Lambda_{\mathrm{low-k}}$. Moreover, when the decimation scale is reduced to $p_{\max}$, all realistic NN interactions merge to a nearly universal potential, thereby removing the model dependence related to the high momentum components. The method for constructing such low-momentum interactions is as follows.

One begins with the half-on-shell T-matrix for free NN scattering in a given partial wave,

$$T(p',p) = V_{NN}(p',p) + \frac{2}{\pi}\mathcal{P}\int_0^\infty \frac{V_{NN}(p',q)T(q,p)}{p^2-q^2}q^2dq, \tag{5}$$

and introduces a low-momentum half-on-shell T-matrix at the scale $\Lambda_{\mathrm{low-k}}$

$$T_{\mathrm{low-k}}(p',p) = V_{\mathrm{low-k}}(p',p) + \frac{2}{\pi}\mathcal{P}\int_0^{\Lambda_{\mathrm{low-k}}} \frac{V_{\mathrm{low-k}}(p',q)T_{\mathrm{low-k}}(q,p)}{p^2-q^2}q^2dq, \tag{6}$$

where $\mathcal{P}$ denotes the principal value. Since one has to preserve low-energy observables, e.g. scattering phase shifts defined through $\tan\delta(p) = -p\,T(p,p)$, one requires that

$$T_{\mathrm{low-k}}(p',p) = T(p',p)\,, \quad \text{for} \quad p',p < \Lambda_{\mathrm{low-k}}. \tag{7}$$

Eqs. (6) and (7) together define the low-momentum NN interaction $V_{\mathrm{low-k}}$ (for a review see ref. [37]). Under the scale decimation procedure, all high-precision NN potentials flow, as

$\Lambda_{\rm low-k} \to 2.1$ fm^{-1}, to a nearly unique low-momentum potential $V_{\rm low-k}$. In the present study we employ the (bare) chiral N^{3}LO interaction and evolve it down to a resolution scale $\Lambda_{\rm low-k} = 2.1$ fm^{-1}.

As demonstrated in ref. [10] the addition of three-nucleon forces is essential for obtaining reasonable saturation properties of nuclear matter when using the universal low-momentum NN potential $V_{\rm low-k}$ in Hartree-Fock calculations. The construction of decimated low-momentum three-body forces consistent with the two-body decimation for $V_{\rm low-k}$ remains a challenge. The difficulty has so far been addressed pragmatically by exploiting that low-energy nuclear observables must be scale-independent. Following this reasoning the low-energy constants associated with the one-pion exchange component $c_D(\Lambda_{\rm low-k})$ and the short-range contact term $c_E(\Lambda_{\rm low-k})$ of the chiral three-nucleon interaction have been fitted to experimental binding energies of three- and four-nucleon systems (^{3}H, ^{3}He, and ^{4}He) at a given (variable) low-momentum scale $\Lambda_{\rm low-k}$. Since we investigate the density-dependent two-nucleon interaction at the scale $\Lambda_{\rm low-k} = 2.1$ fm^{-1}, we use the corresponding values for c_D and c_E obtained in ref. [38]:

$$c_D(2.1 \text{ fm}^{-1}) = -2.062\,, \qquad c_E(2.1 \text{ fm}^{-1}) = -0.625\,, \tag{8}$$

together with $\Lambda_\chi = 0.7$ GeV. In addition to the low-momentum decimation techniques described above, there exist several other means to construct effective nucleon-nucleon interactions suitable for perturbative many-body calculations, such as the similarity renormalization group transformations [39] and the unitary correlation operator method (UCOM) [40, 41]. The resulting effective two-body interactions are all quantitatively similar, and the inclusion of three-nucleon forces within these different frameworks is currently in progress.

III. IN-MEDIUM NUCLEON-NUCLEON INTERACTION

A. Density-dependent terms in isospin-symmetric nuclear matter

In this section we derive from the leading-order chiral three-nucleon interaction, eqs. (1–4), an effective density-dependent in-medium NN interaction. We are considering the on-shell scattering of two nucleons in isospin-symmetric (spin-saturated) nuclear matter of density $\rho = 2k_f^3/3\pi^2$ in the center-of-mass frame, $N_1(\vec{p}) + N_2(-\vec{p}) \to N_1(\vec{p}+\vec{q}) + N_2(-\vec{p}-\vec{q})$. The kinematics is such that the total momentum of the two-nucleon system is zero in the nuclear matter rest frame before and after the scattering. The magnitude of the in- and out-going nucleon momenta is $p = |\vec{p}| = |\vec{p}+\vec{q}|$, and $q = |\vec{q}|$ is the magnitude of the momentum transfer.

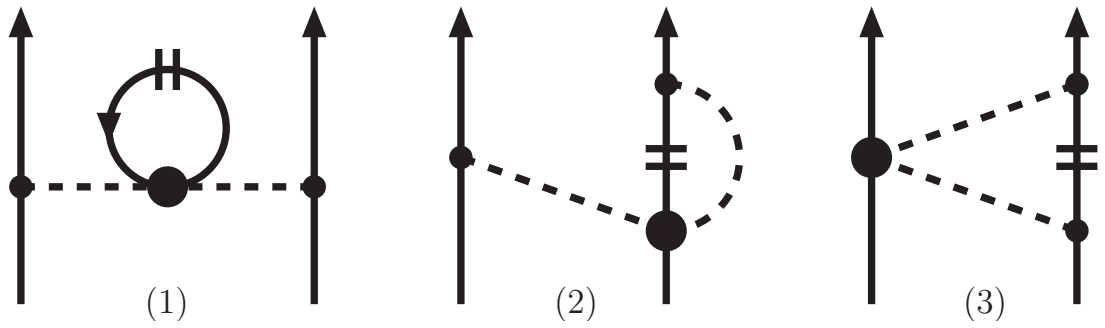

FIG. 2: In-medium NN interaction generated by the two-pion exchange component ($\sim c_{1,3,4}$) of the chiral three-nucleon interaction. The short double-line symbolizes the filled Fermi sea of nucleons, i.e. the medium insertion $-2\pi\delta(k_0)\,\theta(k_f - |\vec{k}\,|)$ in the in-medium nucleon propagator. Reflected diagrams are not shown.

The on-shell interaction in momentum-space has the following (general) form

$$\begin{aligned} V(\vec{p},\vec{q}) \;&=\; V_C + \vec{\tau}_1\cdot\vec{\tau}_2\, W_C + [V_S + \vec{\tau}_1\cdot\vec{\tau}_2\, W_S]\,\vec{\sigma}_1\cdot\vec{\sigma}_2 + [V_T + \vec{\tau}_1\cdot\vec{\tau}_2\, W_T]\,\vec{\sigma}_1\cdot\vec{q}\,\vec{\sigma}_2\cdot\vec{q} \\ &+\; [V_{SO} + \vec{\tau}_1\cdot\vec{\tau}_2\, W_{SO}]\; i(\vec{\sigma}_1+\vec{\sigma}_2)\cdot(\vec{q}\times\vec{p}) \\ &+\; [V_Q + \vec{\tau}_1\cdot\vec{\tau}_2\, W_Q]\;\vec{\sigma}_1\cdot(\vec{q}\times\vec{p})\,\vec{\sigma}_2\cdot(\vec{q}\times\vec{p}). \end{aligned} \tag{9}$$

The subscripts refer to the central (C), spin-spin (S), tensor (T), spin-orbit (SO), and quadratic spin orbit (Q) components of the NN interaction, each of which occurs in an isoscalar (V) and an isovector (W) version. For the purpose of comparison with the density-dependent terms that follow, we reproduce the expression for the (bare) 1π-exchange:

$$V_{NN}^{(1\pi)} = -\frac{g_A^2 M_N}{16\pi f_\pi^2}\vec{\tau}_1\cdot\vec{\tau}_2\,\frac{\vec{\sigma}_1\cdot\vec{q}\,\vec{\sigma}_2\cdot\vec{q}}{m_\pi^2+q^2}\,. \tag{10}$$

Here $\vec{\sigma}_{1,2}$ and $\vec{\tau}_{1,2}$ are the usual spin and isospin operators of the two nucleons. Note that we have included an additional factor of $M_N/4\pi$ in V_{NN} in order to be consistent with the conventions commonly chosen for $V_{\rm low-k}$.

We start with those contributions to the in-medium NN-interaction $V_{NN}^{\rm med}$ that are generated by the 2π-exchange component of the chiral three-nucleon force. The three different topologies for non-vanishing one-loop diagrams are shown in Fig. 2. The short double-line on a nucleon propagator symbolizes the filled Fermi sea of nucleons, which introduces the medium insertion $-2\pi\delta(k_0)\,\theta(k_f - |\vec{k}\,|)$ in the in-medium nucleon propagator. In effect, the medium insertion sums up hole propagation and the absence of particle propagation below the Fermi surface $|\vec{k}\,| < k_f$. The left diagram in Fig. 2 represents a 1π-exchange with a Pauli blocked in-medium pion self-energy and the corresponding contribution to $V_{NN}^{\rm med}$ reads:

$$V_{NN}^{\rm med,1} = \frac{g_A^2 M_N \rho}{8\pi f_\pi^4}\,\vec{\tau}_1\cdot\vec{\tau}_2\,\frac{\vec{\sigma}_1\cdot\vec{q}\,\vec{\sigma}_2\cdot\vec{q}}{(m_\pi^2+q^2)^2}\,(2c_1 m_\pi^2 + c_3 q^2)\,. \tag{11}$$

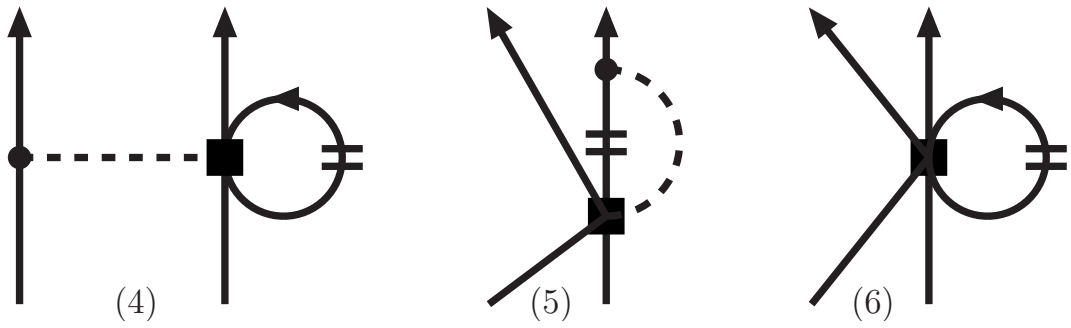

FIG. 3: In-medium NN interaction generated by the one-pion exchange ($\sim c_D$) and short-range component ($\sim c_E$) of the chiral three-nucleon interaction.

Since $c_{1,3} < 0$, this term corresponds to an enhancement of the bare 1π-exchange. It can be interpreted in terms of the reduced pion decay constant, $f_{\pi,s}^{*2} = f_\pi^2 + 2c_3\rho$, that replaces f_π^2 in the denominator of eq. (10) and which is associated with the space components of the axial current in the nuclear medium. The second diagram in Fig. 2 includes vertex corrections to the 1π-exchange caused by Pauli blocking in the nuclear medium. The corresponding contribution to the in-medium NN-interaction has the form:

$$V_{NN}^{\rm med,2} = \frac{g_A^2 M_N}{32\pi^3 f_\pi^4}\vec{\tau}_1\cdot\vec{\tau}_2\,\frac{\vec{\sigma}_1\cdot\vec{q}\,\vec{\sigma}_2\cdot\vec{q}}{m_\pi^2+q^2}\Big\{-4c_1m_\pi^2\Big[\Gamma_0(p)+\Gamma_1(p)\Big] \\ -(c_3+c_4)\Big[q^2\Big(\Gamma_0(p)+2\Gamma_1(p)+\Gamma_3(p)\Big)+4\Gamma_2(p)\Big]+4c_4\Big[\frac{2k_f^3}{3}-m_\pi^2\Gamma_0(p)\Big]\Big\}\,. \quad (12)$$

Here, we have introduced the k_f-dependent functions $\Gamma_j(p)$ which result from Fermi sphere integrals, $\int_{|\vec{k}|\le k_f} d^3k$, over a static pion-propagator $[m_\pi^2+(\vec{k}+\vec{p})^2]^{-1}$:

$$\Gamma_0(p) = k_f - m_\pi\Big[\arctan\frac{k_f+p}{m_\pi}+\arctan\frac{k_f-p}{m_\pi}\Big]+\frac{m_\pi^2+k_f^2-p^2}{4p}\ln\frac{m_\pi^2+(k_f+p)^2}{m_\pi^2+(k_f-p)^2}\,, \quad (13)$$

$$\Gamma_1(p) = \frac{k_f}{4p^2}(m_\pi^2+k_f^2+p^2)-\Gamma_0(p)-\frac{1}{16p^3}\Big[m_\pi^2+(k_f+p)^2\Big]\Big[m_\pi^2+(k_f-p)^2\Big]\ln\frac{m_\pi^2+(k_f+p)^2}{m_\pi^2+(k_f-p)^2}\,, \quad (14)$$

$$\Gamma_2(p) = \frac{k_f^3}{9}+\frac{1}{6}(k_f^2-m_\pi^2-p^2)\Gamma_0(p)+\frac{1}{6}(m_\pi^2+k_f^2-p^2)\Gamma_1(p)\,, \quad (15)$$

$$\Gamma_3(p) = \frac{k_f^3}{3p^2}-\frac{m_\pi^2+k_f^2+p^2}{2p^2}\Gamma_0(p)-\frac{m_\pi^2+k_f^2+3p^2}{2p^2}\Gamma_1(p)\,. \quad (16)$$

By analyzing the momentum and density dependent factor in eq. (12) relative to $V_{NN}^{(1\pi)}$, one finds that this contribution corresponds to a reduction of the 1π-exchange in the nuclear medium. Approximately, this feature can be interpreted in terms of a reduced nucleon axial-vector constant g_A^*.

The right diagram in Fig. 2 represents Pauli blocking effects on chiral 2π-exchange. Evaluating it together with the reflected diagram one finds the following contribution to the in-medium

NN-interaction:

$$
\begin{aligned}
V_{NN}^{\rm med,3} \;=\; & \frac{g_A^2 M_N}{64\pi^3 f_\pi^4}\Big\{ -12c_1 m_\pi^2\Big[2\Gamma_0(p) - (2m_\pi^2+q^2)G_0(p,q)\Big] \\
& -c_3\Big[8k_f^3 - 12(2m_\pi^2+q^2)\Gamma_0(p) - 6q^2\Gamma_1(p) + 3(2m_\pi^2+q^2)^2 G_0(p,q)\Big] \\
& +4c_4\,\vec\tau_1\cdot\vec\tau_2\,(\vec\sigma_1\cdot\vec\sigma_2\,q^2 - \vec\sigma_1\cdot\vec q\,\vec\sigma_2\cdot\vec q)G_2(p,q) \\
& -(3c_3 + c_4\vec\tau_1\cdot\vec\tau_2)\,i(\vec\sigma_1+\vec\sigma_2)\cdot(\vec q\times\vec p\,)\Big[2\Gamma_0(p) + 2\Gamma_1(p) - (2m_\pi^2+q^2) \\
& \times\Big(G_0(p,q) + 2G_1(p,q)\Big)\Big] - 12c_1 m_\pi^2\, i(\vec\sigma_1+\vec\sigma_2)\cdot(\vec q\times\vec p\,)\Big[G_0(p,q) + 2G_1(p,q)\Big] \\
& +4c_4\,\vec\tau_1\cdot\vec\tau_2\,\vec\sigma_1\cdot(\vec q\times\vec p\,)\,\vec\sigma_2\cdot(\vec q\times\vec p\,)\Big[G_0(p,q) + 4G_1(p,q) + 4G_3(p,q)\Big]\Big\}\,. \qquad (17)
\end{aligned}
$$

One observes that in comparison to the analogous 2π-exchange interaction in vacuum (see section 4.2 in ref. [42]) the Pauli blocking in the nuclear medium has generated additional spin-orbit terms, $i(\vec\sigma_1+\vec\sigma_2)\cdot(\vec q\times\vec p\,)$, and quadratic spin-orbit terms, $\vec\sigma_1\cdot(\vec q\times\vec p\,)\,\vec\sigma_2\cdot(\vec q\times\vec p\,)$, written in the last three lines of eq. (17). The density dependent spin-orbit terms (scaling with $c_{3,4}$) in the in-medium NN-interaction $V_{NN}^{\rm med,3}$ demonstrate clearly and explicitly the mechanism of three-body induced spin-orbit forces proposed long ago by Fujita and Miyazawa [33]. The functions $G_j(p,q)$ appearing in eq. (17) result from Fermi sphere integrals over the product of two different pion-propagators. Performing the angular integrations analytically one arrives at:

$$
G_{0,*,**}(p,q) = \frac{2}{q}\int_0^{k_f} dk\,\frac{\{k,k^3,k^5\}}{\sqrt{A(p)+q^2k^2}}\ln\frac{q\,k+\sqrt{A(p)+q^2k^2}}{\sqrt{A(p)}}\,, \qquad (18)
$$

with the abbreviation $A(p)=[m_\pi^2+(k+p)^2][m_\pi^2+(k-p)^2]$. The other functions with $j=1,2,3$ are obtained by solving a system of linear equations:

$$
\begin{aligned}
G_1(p,q) \;&=\; \frac{\Gamma_0(p) - (m_\pi^2+p^2)G_0(p,q) - G_*(p,q)}{4p^2-q^2}\,, && (19)\\
G_{1*}(p,q) \;&=\; \frac{3\Gamma_2(p) + p^2\Gamma_3(p) - (m_\pi^2+p^2)G_*(p,q) - G_{**}(p,q)}{4p^2-q^2}\,, && (20)\\
G_2(p,q) \;&=\; (m_\pi^2+p^2)G_1(p,q) + G_*(p,q) + G_{1*}(p,q)\,, && (21)\\
G_3(p,q) \;&=\; \frac{\frac{1}{2}\Gamma_1(p) - 2(m_\pi^2+p^2)G_1(p,q) - 2G_{1*}(p,q) - G_*(p,q)}{4p^2-q^2}\,. && (22)
\end{aligned}
$$

In this chain of equations the functions indexed with an asterisk play only an auxiliary role for the construction of $G_{1,2,3}(p,q)$. We note that all functions $G_j(p,q)$ are non-singular at $q=2p$ (corresponding to scattering in backward direction). For notational simplicity, the k_f-dependence of $\Gamma_j(p)$ and $G_j(p,q)$ has been suppressed.

Next, we come to the 1π-exchange component of the chiral three-nucleon interaction proportional to the parameter c_D/Λ_χ, where $c_D \simeq -2$ for a scale of $\Lambda_\chi = 0.7\,\mathrm{GeV}$ [38]. The filled black square in the first and second diagram of Fig. 3 symbolizes the corresponding two-nucleon

one-pion contact interaction. By closing a nucleon line at the contact vertex, one obtains a vertex correction (linear in the density ρ) to the 1π-exchange:

$$V_{NN}^{\rm med,4} = -\frac{g_A M_N c_D \rho}{32\pi f_\pi^4 \Lambda_\chi}\,\vec\tau_1\cdot\vec\tau_2\,\frac{\vec\sigma_1\cdot\vec q\,\vec\sigma_2\cdot\vec q}{m_\pi^2+q^2}\,. \tag{23}$$

Since c_D is negative, this term reduces again the bare 1π-exchange, roughly by about 16% at normal nuclear matter density $\rho_0 = 0.16\,\mathrm{fm}^{-3}$. The second diagram in Fig. 3 includes Pauli blocked (pionic) vertex corrections to the short-range NN interaction. The corresponding contribution to the density dependent in-medium NN interaction reads:

$$\begin{aligned} V_{NN}^{\rm med,5} \;=\; & \frac{g_A M_N c_D}{64\pi^3 f_\pi^4 \Lambda_\chi}\vec\tau_1\cdot\vec\tau_2\Bigg\{2\vec\sigma_1\cdot\vec\sigma_2\,\Gamma_2(p) + \Bigg[\vec\sigma_1\cdot\vec\sigma_2\left(2p^2-\frac{q^2}{2}\right)+\vec\sigma_1\cdot\vec q\,\vec\sigma_2\cdot\vec q\left(1-\frac{2p^2}{q^2}\right) \\ & -\frac{2}{q^2}\,\vec\sigma_1\cdot(\vec q\times\vec p\,)\,\vec\sigma_2\cdot(\vec q\times\vec p\,)\Bigg]\Big[\Gamma_0(p)+2\Gamma_1(p)+\Gamma_3(p)\Big]\Bigg\}\,, \end{aligned} \tag{24}$$

where we have used an identity for $\vec\sigma_1\cdot\vec p\,\vec\sigma_2\cdot\vec p+\vec\sigma_1\cdot(\vec p+\vec q\,)\,\vec\sigma_2\cdot(\vec p+\vec q\,)=[\ldots]$. The ellipses stands for the combination of spin operators written in the square bracket of eq. (24).

Finally, there is the short-range component of the chiral 3N interaction, represented by a three-nucleon contact-vertex proportional to c_E/Λ_χ. By closing one nucleon line (see right diagram in Fig. 2) one obtains the following contribution to the in-medium NN-interaction:

$$V_{NN}^{\rm med,6} = -\frac{3M_N c_E \rho}{8\pi f_\pi^4 \Lambda_\chi}\,, \tag{25}$$

which simply grows linearly in density $\rho = 2k_f^3/3\pi^2$ and is independent of spin, isospin and nucleon momenta [44].

The above expressions have been derived for on-shell scattering, which greatly simplifies the calculation of the density-dependent corrections to the NN interaction. As discussed in ref. [22], a suitable choice for extrapolating these expressions off-shell is to make the substitution $p^2 \to \frac{1}{2}(p^2+p'^2)$. Additionally we include a regulator function of the form $\exp\,[-(p/\Lambda_{\rm low-k})^4-(p'/\Lambda_{\rm low-k})^4]$, where $\Lambda_{\rm low-k} = 2.1$ fm^{-1} is chosen so that the two-body and three-body force contributions are decimated down to the same scale. This is consistent with the approach taken in ref. [38].

B. Correction terms in isospin asymmetric nuclear matter

Now we consider the additional modifications $W_{NN}^{\rm med,i}$ to the six in-medium NN scattering T-matrices, $V_{NN}^{\rm med,i}$, resulting from a small isospin asymmetry. The total nucleon density made up by protons and neutrons is $\rho = \rho_n + \rho_p$, and the Fermi momentum k_f is given as before by the relation $\rho = 2k_f^3/3\pi^2$. As a measure of the isospin asymmetry, we define the relative

neutron excess $\delta_{np} = (\rho_n - \rho_p)/\rho$. For a heavy nucleus such as ^{208}Pb, the relative neutron excess is of the order $\delta_{np} \simeq 0.2$. Re-evaluating the six diagrams in Figs. 2 and 3 with the substitution

$$\begin{aligned}\theta(k_f - |\vec{k}|) \;&\to\; \frac{1+\tau^3}{2}\,\theta(k_f(1-\delta_{np})^{1/3} - |\vec{k}|) + \frac{1-\tau^3}{2}\,\theta(k_f(1+\delta_{np})^{1/3} - |\vec{k}|) \\ &=\; \left(1 - \tau^3\delta_{np}\frac{k_f}{3}\frac{\partial}{\partial k_f}\right)\theta(k_f - |\vec{k}|) + \cdots\,, \end{aligned} \tag{26}$$

we obtain the following expressions for the corrections (linear in δ_{np}) to the density-dependent NN interaction.

$$W_{NN}^{\rm med,1} = 0, \tag{27}$$

$$\begin{aligned} W_{NN}^{\rm med,2} \;=\; & \frac{g_A^2 M_N \delta_{np}}{192\pi^3 f_\pi^4}(\tau_1^3 + \tau_2^3)\,\frac{\vec{\sigma}_1\cdot\vec{q}\,\vec{\sigma}_2\cdot\vec{q}}{m_\pi^2+q^2}\,k_f\frac{\partial}{\partial k_f}\Big\{4c_1 m_\pi^2\Big[\Gamma_0(p)+\Gamma_1(p)\Big] + (c_3-c_4) \\ & \times\Big[q^2\Big(\Gamma_0(p)+2\Gamma_1(p)+\Gamma_3(p)\Big) + 4\Gamma_2(p)\Big] + 4c_4\left[\frac{2k_f^3}{3} - m_\pi^2\Gamma_0(p)\right]\Big\}\,, \end{aligned} \tag{28}$$

$$\begin{aligned} W_{NN}^{\rm med,3} \;=\; & \frac{g_A^2 M_N \delta_{np}}{384\pi^3 f_\pi^4}(\tau_1^3+\tau_2^3)k_f\frac{\partial}{\partial k_f}\Big\{ -4c_1 m_\pi^2\Big[2\Gamma_0(p) - (2m_\pi^2+q^2)G_0(p,q)\Big] \\ & -c_3\Big[\frac{8k_f^3}{3} - 4(2m_\pi^2+q^2)\Gamma_0(p) - 2q^2\Gamma_1(p) + (2m_\pi^2+q^2)^2 G_0(p,q)\Big] \\ & +4c_4\,(\vec{\sigma}_1\cdot\vec{\sigma}_2\,q^2 - \vec{\sigma}_1\cdot\vec{q}\,\vec{\sigma}_2\cdot\vec{q})G_2(p,q) \\ & -(c_3+c_4)\,i(\vec{\sigma}_1+\vec{\sigma}_2)\cdot(\vec{q}\times\vec{p})\Big[2\Gamma_0(p) + 2\Gamma_1(p) - (2m_\pi^2+q^2) \\ & \times\Big(G_0(p,q)+2G_1(p,q)\Big)\Big] - 4c_1 m_\pi^2\,i(\vec{\sigma}_1+\vec{\sigma}_2)\cdot(\vec{q}\times\vec{p})\Big[G_0(p,q)+2G_1(p,q)\Big] \\ & +4c_4\,\vec{\sigma}_1\cdot(\vec{q}\times\vec{p})\,\vec{\sigma}_2\cdot(\vec{q}\times\vec{p})\Big[G_0(p,q)+4G_1(p,q)+4G_3(p,q)\Big]\Big\}\,, \end{aligned} \tag{29}$$

$$W_{NN}^{\rm med,4} = \frac{g_A M_N c_D(\rho_p-\rho_n)}{64\pi f_\pi^4\Lambda_\chi}\,(\tau_1^3+\tau_2^3)\,\frac{\vec{\sigma}_1\cdot\vec{q}\,\vec{\sigma}_2\cdot\vec{q}}{m_\pi^2+q^2}\,, \tag{30}$$

$$\begin{aligned} W_{NN}^{\rm med,5} \;=\; & -\frac{g_A M_N c_D \delta_{np}}{384\pi^3 f_\pi^4\Lambda_\chi}(\tau_1^3+\tau_2^3)k_f\frac{\partial}{\partial k_f}\Big\{2\vec{\sigma}_1\cdot\vec{\sigma}_2\,\Gamma_2(p) + \Big[\vec{\sigma}_1\cdot\vec{\sigma}_2\Big(2p^2 - \frac{q^2}{2}\Big) + \vec{\sigma}_1\cdot\vec{q}\,\vec{\sigma}_2\cdot\vec{q} \\ & \times\Big(1 - \frac{2p^2}{q^2}\Big) - \frac{2}{q^2}\,\vec{\sigma}_1\cdot(\vec{q}\times\vec{p})\,\vec{\sigma}_2\cdot(\vec{q}\times\vec{p})\Big]\Big[\Gamma_0(p)+2\Gamma_1(p)+\Gamma_3(p)\Big]\Big\}\,, \quad \text{and} \end{aligned} \tag{31}$$

$$W_{NN}^{\rm med,6} = \frac{3M_N c_E(\rho_p-\rho_n)}{16\pi f_\pi^4\Lambda_\chi}(\tau_1^3+\tau_2^3)\,. \tag{32}$$

For completeness we also list the derivatives with respect to k_f of the loop functions $\Gamma_j(p)$ and $G_j(p,q)$ encountered in the previous section:

$$\frac{\partial\Gamma_0(p)}{\partial k_f} = \frac{k_f}{2p}\ln\frac{m_\pi^2+(k_f+p)^2}{m_\pi^2+(k_f-p)^2}, \tag{33}$$

$$\frac{\partial\Gamma_1(p)}{\partial k_f} = \frac{k_f^2}{p^2} - \frac{m_\pi^2+k_f^2+p^2}{2p^2}\frac{\partial\Gamma_0(p)}{\partial k_f}, \tag{34}$$

$$\frac{\partial\Gamma_2(p)}{\partial k_f} = \frac{k_f^2}{4p^2}(m_\pi^2+k_f^2+p^2) - \frac{1}{8p^2}\left[m_\pi^2+(k_f+p)^2\right]\left[m_\pi^2+(k_f-p)^2\right]\frac{\partial\Gamma_0(p)}{\partial k_f}, \tag{35}$$

$$\frac{\partial\Gamma_3(p)}{\partial k_f} = \frac{1}{p^2}\left[k_f^2\frac{\partial\Gamma_0(p)}{\partial k_f} - 3\frac{\partial\Gamma_2(p)}{\partial k_f}\right], \tag{36}$$

$$\frac{\partial}{\partial k_f}G_{0,*,**}(p,q) = \frac{2\{k_f,k_f^2,k_f^3\}}{q\sqrt{\tilde{A}(p)+q^2k_f^2}}\ln\frac{qk_f+\sqrt{\tilde{A}(p)+q^2k_f^2}}{\sqrt{\tilde{A}(p)}}, \tag{37}$$

with the abbreviation $\tilde{A}(p) = [m_\pi^2+(k_f+p)^2]\,[m_\pi^2+(k_f-p)^2]$. Aside from the pion self-energy term, which receives no modification linear in the isospin asymmetry, each term $W_{NN}^{\rm med,i}$ is proportional to the factor $(\tau_1^3+\tau_2^3)\,\delta_{np}$. Therefore, the proton-proton (pp) and neutron-neutron (nn) interactions in isospin-asymmetric nuclear matter receive corrections of opposite sign, while the neutron-proton (np) interaction remains unchanged at linear order in δ_{np}. In general, we expect these corrections to be small, though the difference between the in-medium pp and nn interactions can be important as we discuss in the next section.

IV. NUMERICAL RESULTS

A. Partial wave projection

For the purpose of demonstration and for nuclear structure calculations it is convenient to evaluate the above in-medium NN interaction in the partial-wave basis consisting of eigenstates with definite L,S,J quantum numbers. We have followed the detailed description in ref. [43] and obtain with $U_K = V_K + (4I-3)W_K$, $(K = C,S,T,SO,Q)$ the relevant linear combination in a state with total isospin $I = 0,1$ the following projection formulas:

a) Singlet matrix element with $S = 0$ and $L = J$:

$$\langle J0J|V_{NN}|J0J\rangle = \frac{1}{2}\int_{-1}^{1}dz\Big[U_C - 3U_S - q^2U_T + p^4(z^2-1)U_Q\Big]P_J(z)\,. \tag{38}$$

b) Triplet matrix element with $S = 1$ and $L = J$:

$$\begin{aligned}\langle J1J|V_{NN}|J1J\rangle = \frac{1}{2}\int_{-1}^{1}dz\Big\{&2p^2\Big[U_{SO} - U_T + p^2zU_Q\Big]\Big(P_{J+1}(z)+P_{J-1}(z)\Big)\\ &+\Big[U_C + U_S + 2p^2(1+z)U_T - 4p^2zU_{SO} - p^4(3z^2+1)U_Q\Big]P_J(z)\Big\}\,.\end{aligned} \tag{39}$$

c) Triplet matrix elements with $S = 1$ and $L = J \pm 1$:

$$\langle J \pm 1, 1J | V_{NN} | J \pm 1, 1J \rangle = \frac{1}{2} \int_{-1}^{1} dz \Big\{ 2p^2 \Big[U_{SO} \pm \frac{1}{2J+1} \Big(U_T - p^2 z U_Q \Big) \Big] P_J(z) + \Big[U_C + U_S + p^2 \Big(p^2 (1-z^2) U_Q - 2z U_{SO} \pm \frac{2}{2J+1} \Big(p^2 U_Q - U_T \Big) \Big) \Big] P_{J\pm1}(z) \Big\} . \quad (40)$$

d) Triplet mixing matrix element with $S = 1$, $L' = J - 1$ and $L = J + 1$:

$$\langle J-1, 1J | V_{NN} | J+1, 1J \rangle = \frac{\sqrt{J+1} p^2}{\sqrt{J}(2J+1)} \int_{-1}^{1} dz \Big\{ \Big(U_T - p^2 U_Q \Big) P_{J+1}(z) + \Big[\big(2J - z(2J+1) \big) U_T + p^2 z U_Q \Big] P_J(z) \Big\} . \quad (41)$$

Here, $P_J(z)$ are ordinary Legendre polynomials of degree J and the momentum transfer q is set to $q = p\sqrt{2(1-z)}$. The resulting partial wave amplitudes are now functions of the momentum p and k_f (or equivalently the nucleon density ρ). Note that the off-diagonal mixing matrix elements arise exclusively from the tensor operator $\vec{\sigma}_1 \cdot \vec{q}\, \vec{\sigma}_2 \cdot \vec{q}$ and the quadratic spin-orbit operator $\vec{\sigma}_1 \cdot (\vec{q} \times \vec{p})\, \vec{\sigma}_2 \cdot (\vec{q} \times \vec{p})$.

B. S-waves and $S - D$ mixing

In Figs. 4 and 5 we show by the solid lines the (diagonal) partial-wave amplitudes of $V_{\mathrm{low-k}}$ in the channels $^1\mathrm{S}_0$, $^3\mathrm{S}_1$, and $^3\mathrm{D}_1$ as well as the $^3\mathrm{S}_1 - ^3\mathrm{D}_1$ mixing matrix element for a cutoff $\Lambda_{\mathrm{low-k}} = 2.1$ fm^{-1}. We also show the modification of the low-momentum interaction due to the six different components of the density-dependent NN interaction derived from the leading-order chiral three-nucleon force in an isospin symmetric nuclear medium with density $\rho = \rho_0$. The pion self-energy correction $V_{NN}^{\mathrm{med},1}$ and the Pauli-blocked one-pion exchange vertex correction $V_{NN}^{\mathrm{med},2}$, which both arise from the long-range three-nucleon force, vanish as $q \to 0$ and therefore give no modification to the S-wave amplitudes as $p \to 0$. Moreover, to a large extent they contribute with opposite sign and equal strength. Consequently, their combined effect on the S-wave amplitudes is rather small. In comparison, the long-range Pauli-blocked 2π-exchange term $V_{NN}^{\mathrm{med},3}$ contributes strongly to the S waves at large distances (small momenta) and has little effect at short distances (large momenta). In fact, Pauli-blocked 2π-exchange is the dominant mechanism for suppressing the S-wave attraction at low momenta. From Fig. 5 we observe that the contributions $V_{NN}^{\mathrm{med},4}$ and $V_{NN}^{\mathrm{med},5}$, resulting from the medium-range three-nucleon force proportional to c_D, are naturally small in S-waves. Additionally, they enter with opposite sign and therefore play a very minor role in modifying the S-wave interaction. The final contribution $V_{NN}^{\mathrm{med},6}$ comes from the three-nucleon contact interaction proportional to c_E.

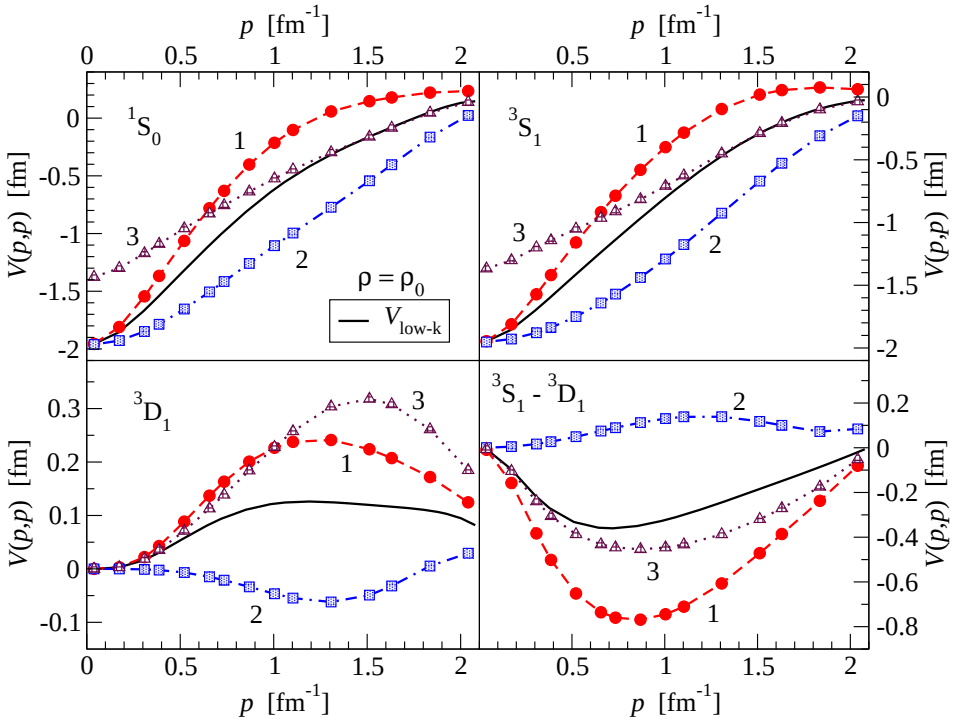

FIG. 4: Modifications to the ^{1}S$_0$, ^{3}S$_1$, ^{3}D$_1$, and ^{3}S$_1$–^{3}D$_1$ partial wave amplitudes of $V_{\rm low-k}$ (shown by the solid curve) due to the first three density-dependent contributions $V_{NN}^{\rm med;\,1,2,3}$ at nuclear matter saturation density $\rho_0 = 0.16$ fm^{-3}.

Since it is independent of the momentum p (aside from the suppression above $p = 1.5$ fm^{-1} due to the regulator function), it affects only the two S-waves. In combination with $V_{NN}^{\rm med,3}$ it plays a major role in reducing the S-wave NN attraction in the nuclear medium.

In the ^{3}D$_1$ partial wave we find again that the pion self-energy correction $V_{NN}^{\rm med,1}$ largely cancels the effect from the long-range Pauli-blocked vertex correction $V_{NN}^{\rm med,2}$. The Pauli-blocked 2π-exchange contribution $V_{NN}^{\rm med,3}$ now vanishes at small momenta and has a large effect at high momenta, in contrast to its role in the S-waves. By itself, $V_{NN}^{\rm med,3}$ would nearly double the repulsion in the ^{3}D$_1$ channel. This enhancement of the ^{3}D$_1$ repulsion is reduced in part by the attractive contribution coming from the medium-range Pauli-blocked one-pion-exchange vertex correction $V_{NN}^{\rm med,4}$. The final possible contribution, $V_{NN}^{\rm med,5}$, in this channel is negligible. Finally, the ^{3}S$_1$–^{3}D$_1$ mixing matrix element receives contributions from all density-dependent terms except the short-range contact interaction $V_{NN}^{\rm med,6}$ since each of the first five contributions includes a tensor component. Only $V_{NN}^{\rm med,2}$ and $V_{NN}^{\rm med,4}$ give repulsive contributions to the ^{3}S$_1$–^{3}D$_1$ mixing, and these terms are generally weaker than the three attractive contributions.

In Fig. 6 we show the modifications of the momentum-space matrix elements in the ^{1}S$_0$, ^{3}S$_1$, and ^{3}D$_1$ partial waves of $V_{\rm low-k}$ due to all density-dependent contributions. The complete

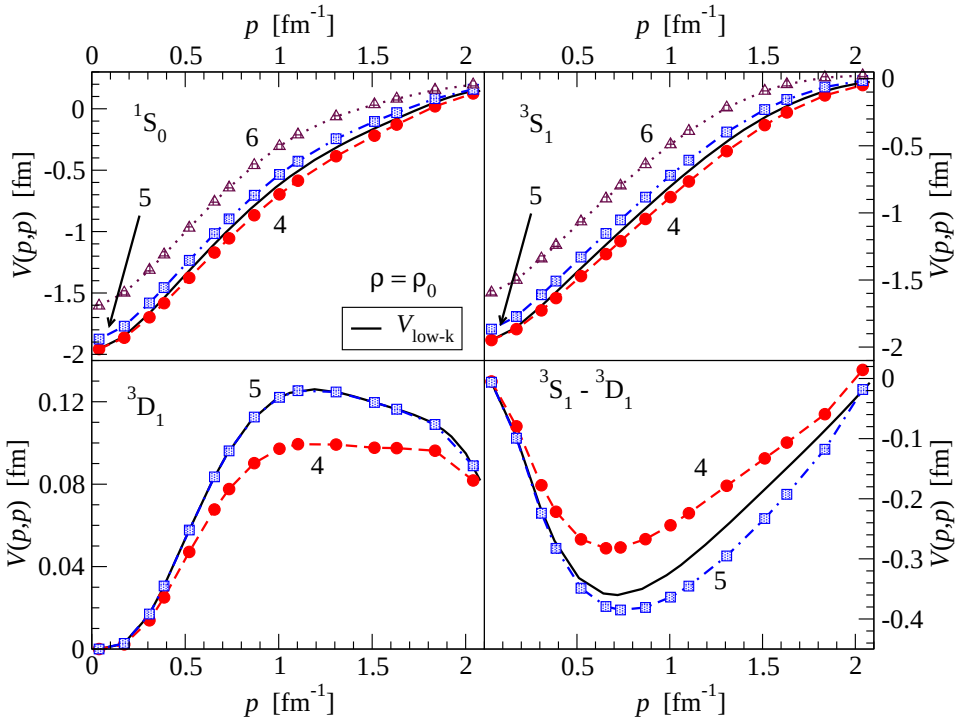

FIG. 5: Modifications to the $^1S_0$, $^3S_1$, $^3D_1$, and $^3S_1-^3D_1$ partial wave amplitudes of $V_{\rm low-k}$ (shown by the solid curve) due to the three density-dependent contributions $V_{NN}^{\rm med;\,4,5,6}$ at nuclear matter saturation density $\rho_0 = 0.16$ fm^{-3}.

interaction is shown at the densities $\rho_0/2$ and ρ_0. The overall effect is to decrease the strong attraction in S-waves and to increase the repulsion in the (diagonal) $^3D_1$ channel. The $^3S_1-^3D_1$ mixing matrix element becomes on average only mildly more attractive. The repulsive effects increase with the nuclear density and this way provide the mechanism for nuclear matter saturation when using the low-momentum interaction $V_{\rm low-k}$ [10]. Finally, in Fig. 7 we plot the in-medium pp interaction at nuclear matter saturation density ρ_0 for isospin asymmetries $\delta_{np} = \pm 0.2$, where $\delta_{np} = 0.2$ corresponds to the asymmetry reached in heavy nuclei. For larger isospin asymmetries, the effects scale linearly with δ_{np}. We plot as well the results for $\delta_{np} = -0.2$, which corresponds to the nn interaction in a medium with $\delta_{np} = 0.2$. As discussed in Section III B the effects on the pp interaction and nn interaction are equal and of opposite sign. Although the effects due to an isospin asymmetry are in general small, the difference between the pp and nn interactions can be significant, particularly in the $^3S_1$ channel.

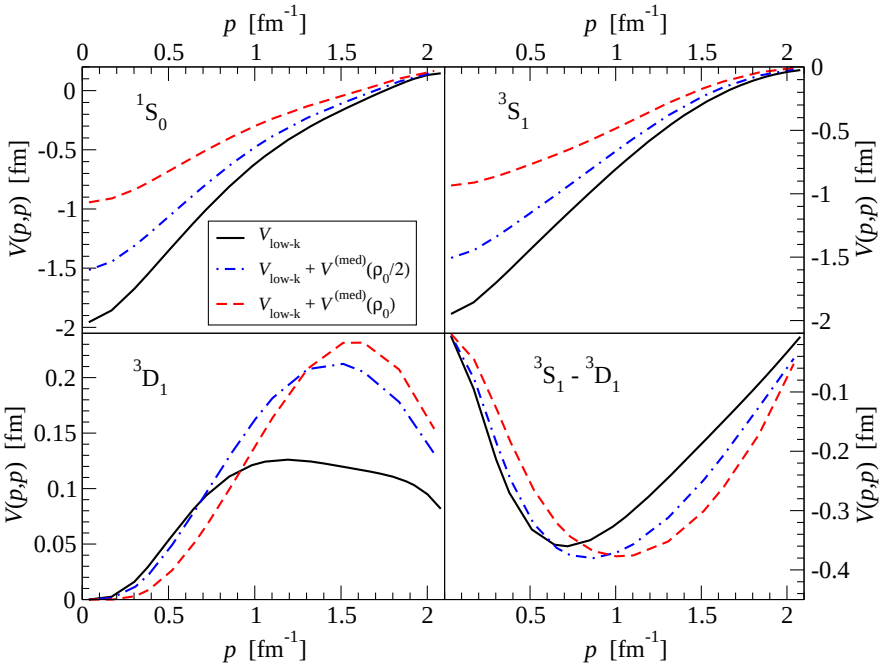

FIG. 6: Dependence of the low-momentum in-medium NN interaction on the nuclear density ρ. Shown are the momentum space matrix elements in the $^1S_0$, $^3S_1$, and $^3D_1$ partial waves and the $^3S_1$–$^3D_1$ mixing matrix element.

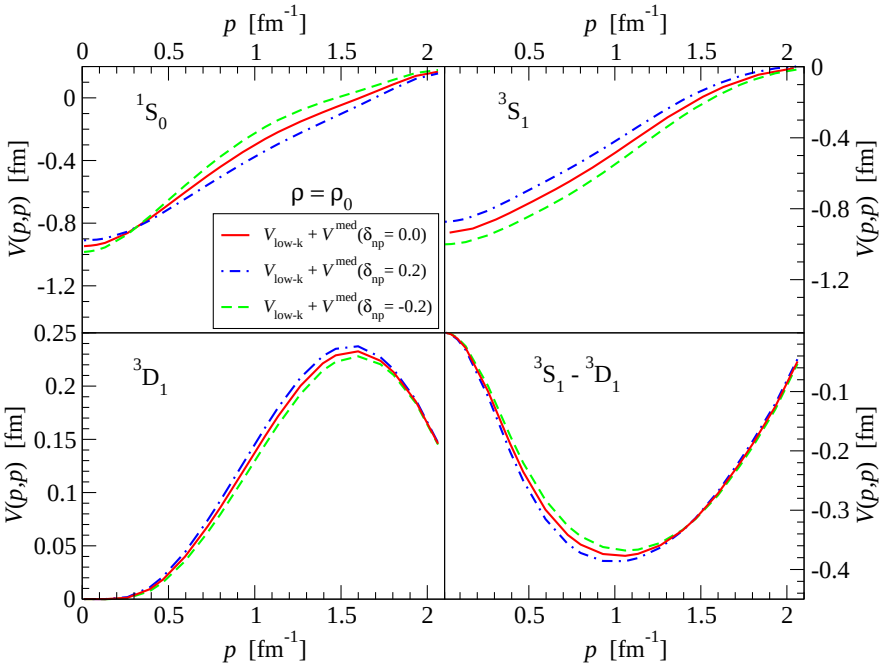

FIG. 7: Dependence of the low-momentum in-medium nucleon-nucleon interaction on the isospin asymmetry $\delta_{np} = (\rho_n - \rho_p)/\rho$ at $\rho_0 = 0.16$ fm^{-3}. Shown are the momentum space matrix elements in the $^1S_0$, $^3S_1$, and $^3D_1$ partial waves and the $^3S_1$–$^3D_1$ mixing matrix element.

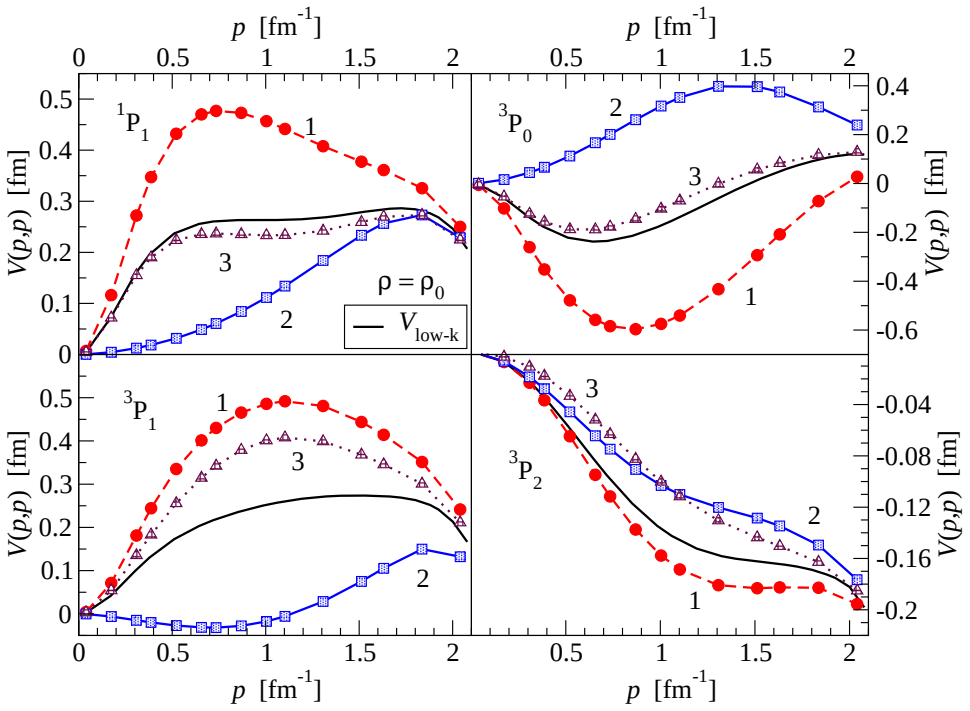

FIG. 8: Modifications to the ^{1}P$_1$, ^{3}P$_0$, ^{3}P$_1$, and ^{3}P$_2$ partial wave amplitudes of $V_{\rm low-k}$ (denoted by the solid line) due to the first three density-dependent contributions $V_{NN}^{\rm med;\,1,2,3}$ at a nuclear density $\rho = \rho_0$.

C. *P*-waves

There are three uncoupled $L = 1$ partial waves, namely ^{1}P$_1$, ^{3}P$_0$, and ^{3}P$_1$, as well as the ^{3}P$_2$ partial wave which can couple through the tensor and quadratic spin-orbit forces to the ^{3}F$_2$ partial wave. In Figs. 8 and 9 we have plotted the effects of the six components of the density-dependent NN interaction on each of these P-wave amplitudes. We consider a medium of isospin-symmetric nuclear matter at saturation density ρ_0. Again we find that although the pion self-energy correction and the long-range one-pion-exchange vertex correction are the largest contributions in all channels, taken together they have only a moderate effect. The Pauli-blocked two-pion exchange contribution $V_{NN}^{\rm med,3}$ is attractive in the P-wave spin-singlet states and repulsive in spin-triplet states, though only in the ^{3}P$_1$ and ^{3}P$_2$ does it play a significant role. Effects from the one-pion exchange vertex correction arising from the medium-range three-nucleon force ($V_{NN}^{\rm med,4}$) can be as large as 20%, but those from the vertex-corrected short-range nuclear force ($V_{NN}^{\rm med,5}$) are negligible.

In Fig. 10 we have plotted the complete P-wave interactions at densities $\rho_0/2$ and ρ_0. Aside from the ^{3}P$_1$ channel, which on average receives a small attractive contribution from the sum of

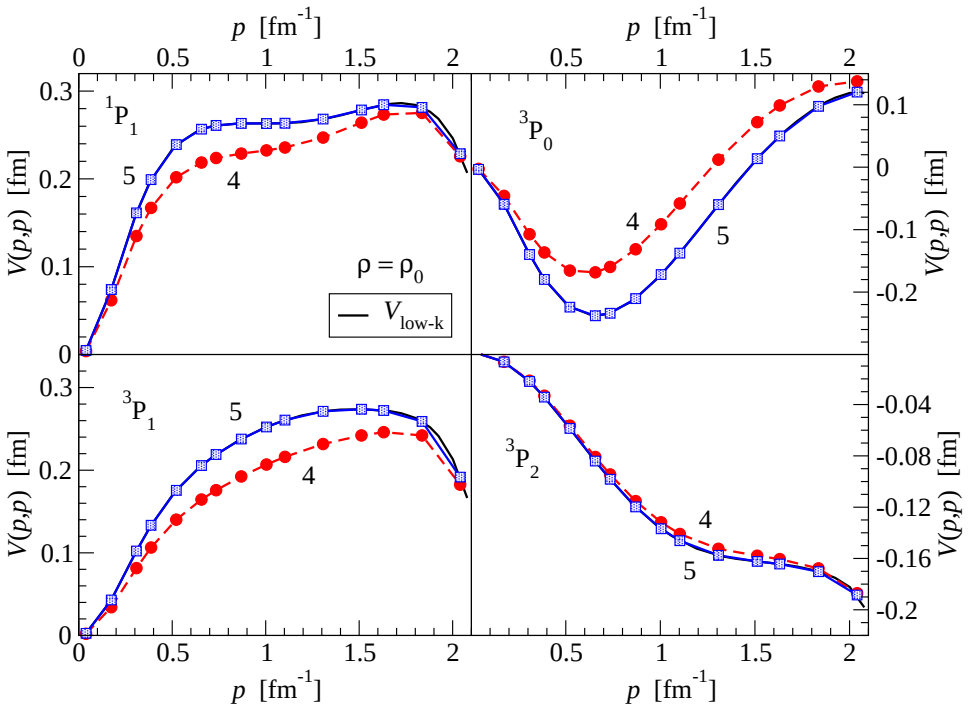

FIG. 9: Modifications to the ^{1}P$_1$, ^{3}P$_0$, ^{3}P$_1$, and ^{3}P$_2$ partial wave amplitudes of $V_{\rm low-k}$ (shown by the solid line) due to $V_{NN}^{\rm med;\,4,5}$ at a nuclear density $\rho = \rho_0$.

the six density-dependent terms, we see that the remaining $L = 1$ partial waves all receive a net repulsive contribution. The ^{3}P$_0$ partial wave is particularly sensitive to these modifications; at nuclear matter saturation density, nearly all of the attraction at small momenta vanishes and the repulsion at higher momenta is largely increased. This results primarily from the repulsion due to $V_{NN}^{\rm med,2}$, $V_{NN}^{\rm med,3}$, and $V_{NN}^{\rm med,4}$. The ^{3}P$_1$ and ^{3}P$_2$ partial waves are less sensitive to the density dependent terms. The ^{3}P$_1$ channel receives two attractive ($V_{NN}^{\rm med,2}$, $V_{NN}^{\rm med,4}$) and two repulsive ($V_{NN}^{\rm med,1}$, $V_{NN}^{\rm med,3}$) modifications which give rise to only a small net repulsive effect limited to intermediate momenta. Finally, for the ^{3}P$_2$ partial wave, only $V_{NN}^{\rm med,1}$, $V_{NN}^{\rm med,2}$, and $V_{NN}^{\rm med,3}$ are important. The net repulsion from $V_{NN}^{\rm med,2}$ and $V_{NN}^{\rm med,3}$ is approximately twice as large as the small attraction from $V_{NN}^{\rm med,1}$. Isospin asymmetry effects ($\delta_{np} = \pm 0.2$) in the $L = 1$ partial waves are shown in Fig. 11. The largest effect is in the ^{3}P$_0$ channel where the difference between the pp and nn interaction is approximately 25% of the total interaction strength. In fact, in the pp channel there is almost no attraction remaining.

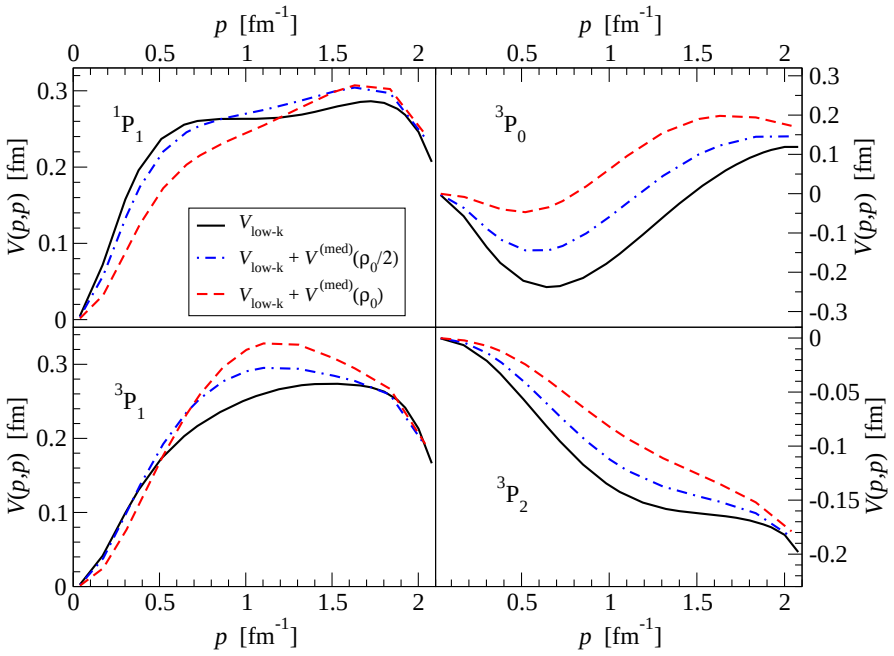

FIG. 10: Dependence of the low-momentum in-medium nucleon-nucleon interaction on the nuclear density ρ. Shown are the momentum space matrix elements in the ^{1}P$_1$, ^{3}P$_0$, ^{3}P$_1$, and ^{3}P$_2$ partial waves.

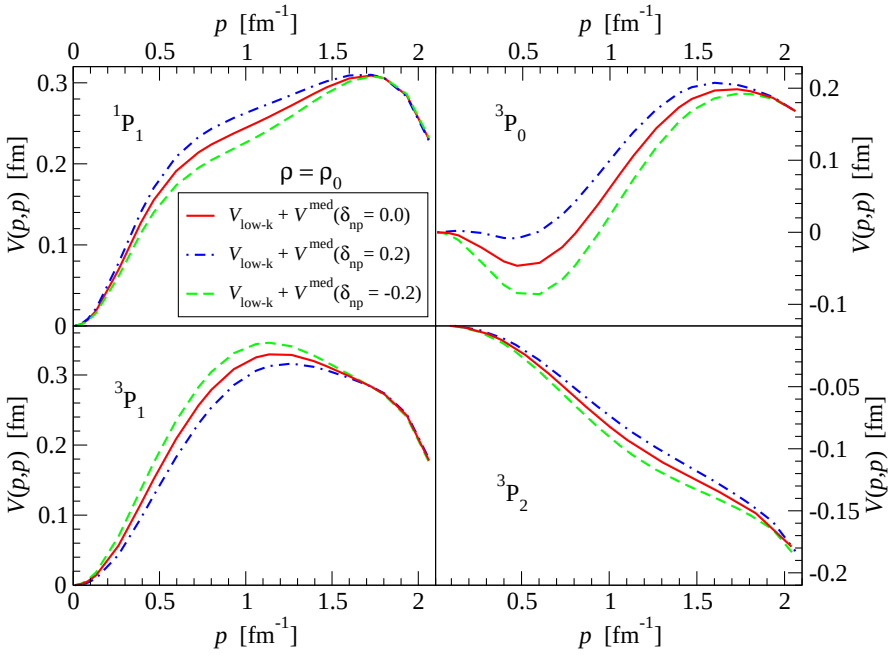

FIG. 11: Dependence of the low-momentum in-medium nucleon-nucleon interaction on the isospin asymmetry $\delta_{np} = (\rho_n - \rho_p)/\rho$ at $\rho_0 = 0.16$ fm^{-3}. Shown are the momentum space matrix elements in the ^{1}P$_1$, ^{3}P$_0$, ^{3}P$_1$, and ^{3}P$_2$ partial waves.

D. D-waves and $D-G$ mixing

Although the remaining $L = 2$ partial waves are mostly smaller by an order of magnitude than the $L = 0$ and 1 partial waves, it is important to see whether the trends observed in the lower partial waves continue. In Figs. 12 and 13 we have plotted the effects from the five (nonvanishing) density-dependent contributions in the ^{1}D$_2$, ^{3}D$_2$, and ^{3}D$_3$ partial waves. As in the S and P-waves, the $V_{NN}^{\rm med,1}$ and $V_{NN}^{\rm med,2}$ terms contribute strongest and with opposite sign. The long-range Pauli-blocked 2π-exchange contribution $V_{NN}^{\rm med,3}$ has little effect, except in the ^{1}D$_2$ partial wave where it gives rise to a strong repulsion. Together with $V_{NN}^{\rm med,2}$, the Pauli-blocked 2π-exchange contribution gives rise to a repulsion in this channel that is significantly larger than the attractive contribution from the pion self energy term $V_{NN}^{\rm med,1}$. In fact, both $V_{NN}^{\rm med,2}$ and $V_{NN}^{\rm med,4}$ are repulsive in all of these channels, except in the ^{3}D$_3$ partial wave where they combine to generate an overall attraction. These results can be seen from Fig. 14 in which we have plotted the complete interaction at densities $\rho_0/2$ and ρ_0. From this figure one can see that all $L = 2$ partial waves, except the ^{3}D$_3$ channel, become less attractive due to the density-dependent corrections. In Fig. 15 we show the effect of an isospin asymmetry on these partial wave amplitudes for $\delta_{np} = \pm 0.2$. Again, we find that in general the modifications are small, though in some channels, such as ^{1}D$_2$, the difference between the pp and nn interactions cannot be neglected.

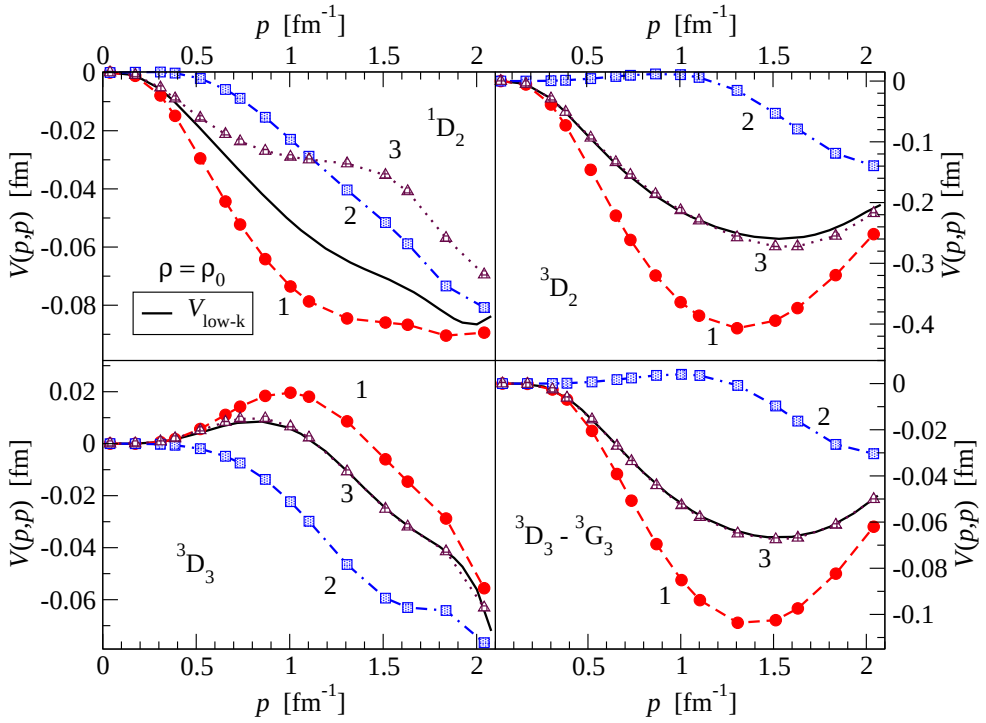

FIG. 12: Modifications to the ^{1}D$_2$, ^{3}D$_2$ and ^{3}D$_3$ partial wave amplitudes and the ^{3}D$_3$−^{3}G$_3$ mixing matrix element of $V_{\rm low-k}$ (shown by the solid line) due to the first three density-dependent contributions $V_{NN}^{\rm med;\,1,2,3}$ at saturation density ρ_0.

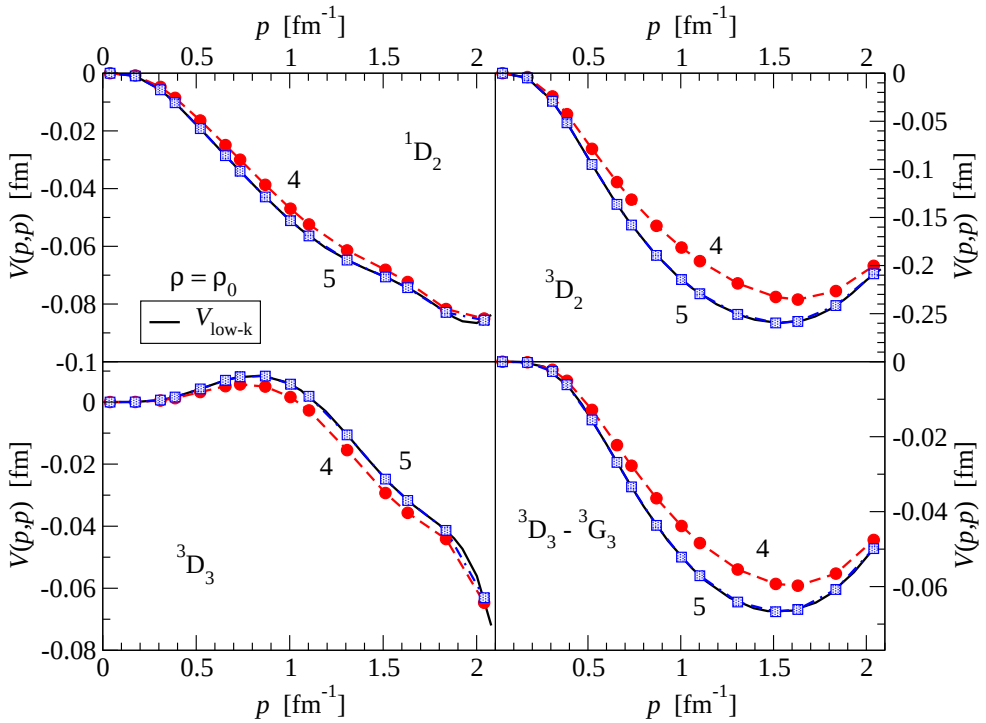

FIG. 13: Modifications to the ^{1}D$_2$, ^{3}D$_2$ and ^{3}D$_3$ partial wave amplitudes and the ^{3}D$_3$−^{3}G$_3$ mixing matrix element of $V_{\rm low-k}$ (shown by the solid line) due to $V_{NN}^{\rm med;\,4,5}$ at saturation density ρ_0.

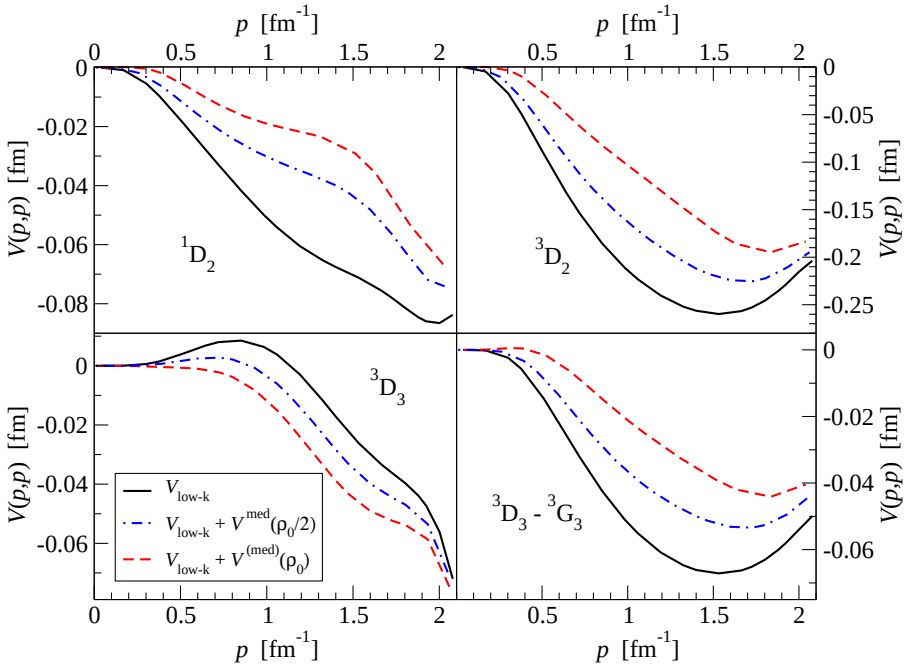

FIG. 14: Dependence of the low-momentum in-medium nucleon-nucleon interaction on the nuclear density ρ. Shown are the momentum space matrix elements in the $^1D_2$, $^3D_2$ and $^3D_3$ partial waves as well as the $^3D_3$–$^3G_3$ mixing matrix element.

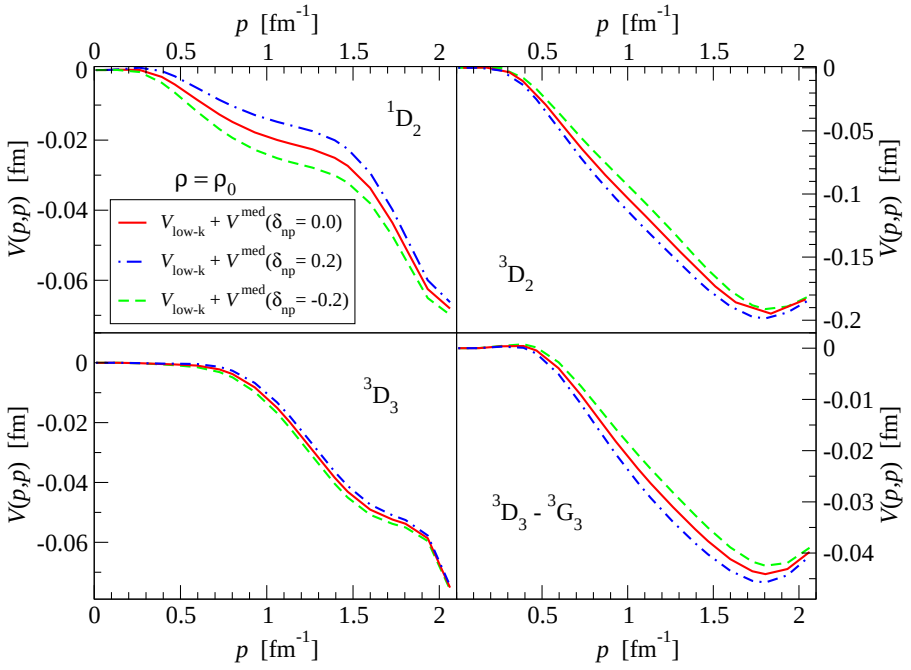

FIG. 15: Dependence of the low-momentum in-medium NN interaction on the isospin asymmetry $\delta_{np} = (\rho_n - \rho_p)/\rho$ at $\rho_0 = 0.16$ fm^{-3}. Shown are the momentum space matrix elements in the $^1D_2$, $^3D_2$ and $^3D_3$ channels and the $^3D_3$–$^3G_3$ mixing matrix element.

V. SUMMARY AND CONCLUSIONS

Using chiral effective field theory, we have derived in this work density-dependent corrections to the nucleon-nucleon interaction in isospin-symmetric as well as isospin-asymmetric nuclear matter. These corrections have been calculated from the six one-loop in-medium NN-scattering diagrams generated by the leading-order chiral three-nucleon interaction. The resulting in-medium NN interaction has been transformed into the $|LSJ\rangle$ basis. Although we have combined the density-dependent corrections with the low-momentum NN potential $V_{\mathrm{low-k}}$ at a selected cutoff $\Lambda_{\mathrm{low-k}} = 2.1$ fm^{-1}, the analytic expressions for the density-dependent terms should hold at any resolution scale by re-adjusting the values of the running low-energy constants $c_D(\Lambda_{\mathrm{low-k}})$ and $c_E(\Lambda_{\mathrm{low-k}})$. In the present work the values of the two low-energy constants $c_D = -2.06$ and $c_E = -0.63$ were taken from a previous calculation [38] of $A = 3, 4$ binding energies using the low-momentum NN potential $V_{\mathrm{low-k}}$ at $\Lambda_{\mathrm{low-k}} = 2.1$ fm^{-1}.

After projecting the interaction into partial waves, we find that the largest density-dependent corrections come from the long-range Pauli-blocked pion self-energy and vertex correction. However, to a large extent they cancel in all partial waves studied and thus give rise to effects comparable to the remaining density-dependent corrections. The two contributions from the medium-range three-nucleon force proportional to c_D are small and generally play only a minor role. In contrast to this, the long-range Pauli-blocked 2π-exchange as well as the contact interaction proportional to c_E provide significant repulsion in most partial waves. The latter acts only in S-waves where it decreases the attraction in the spin-singlet and spin-triplet channels by approximately 20%. In fact, the net effect of all density-dependent corrections is repulsive in nearly all partial waves channels we studied. The repulsive effects increase with density and in this way provide a mechanism for nuclear matter saturation [10]. The repulsive (stabilizing) nature of the pion-induced three-body forces is also observed in the chiral perturbation theory calculation of nuclear matter in ref. [31].

Furthermore, we have found that additional medium modifications due to a (small) isospin asymmetry are present only in the pp and nn channels and are generally small. However, the resulting difference between the in-medium pp and nn interactions can be significant in certain partial waves. This work should serve as a foundation for future nuclear structure calculations exploiting density-dependent chiral effective two-nucleon interactions.

[1] B. D. Day, Rev. Mod. Phys. **39** (1967) 719.

[2] H. Q. Song, M. Baldo, G. Giansiracusa, and U. Lombardo, Phys. Rev. Lett. **81** (1998) 1584.

[3] B. D. Day, Rev. Mod. Phys. **50** (1978) 495.

[4] I. E. Lagaris and V. R. Pandharipande, Nucl. Phys. **A359** (1981) 331; **A359** (1981) 349.

[5] S. D. Yang, J. Heyer, and T. T. S. Kuo, Nucl. Phys. **A448** (1986) 420.

[6] H. Q. Song, S. D. Yang and T. T. S. Kuo, Nucl. Phys. **A462** (1987) 491.

[7] R. Brockmann and R. Machleidt, Phys. Rev. C **42** (1990) 1965.

[8] E. N. E. van Dalen and H. Müther, arXiv:0904.2663.

[9] R. B. Wiringa, V. Fiks, and A. Fabrocini, Phys. Rev. C 38 (1988) 1010.

[10] S. K. Bogner, A. Schwenk, R. J. Furnstahl, and A. Nogga, *Nucl. Phys.* **A763** (2005) 59; and refs. therein.

[11] R. Rapp, R. Machleidt, J. W. Durso, and G. E. Brown, Phys. Rev. Lett. **82** (1999) 1827.

[12] L.-W. Siu, J. W. Holt, T. T. S. Kuo, and G. E. Brown, Phys. Rev. C **79** (2009) 054004.

[13] J. Carlson, Phys. Rev. C **36** (1987) 2026.

[14] J. L. Friar, G. L. Payne, V. G. J. Stoks, and J. J. de Swart, Phys. Lett. B **311** (1993) 4.

[15] A. Nogga, H. Kamada, and W. Glöckle, Phys. Rev. Lett. **85** (2000) 944.

[16] S. C. Pieper, K. Varga, and R. B. Wiringa, Phys. Rev. C **66** (2002) 044310.

[17] P. Navratil, V. G. Gueorguiev, J. P. Vary, W. E. Ormand, and A. Nogga, Phys. Rev. Lett. **99** (2007) 042501.

[18] N. Sakamoto *et al.*, Phys. Lett. B **367** (1996) 60.

[19] H. Sakai *et al.*, Phys. Rev. Lett. **84** (2000) 5288.

[20] H. Witala *et al.*, Phys. Rev. Lett. **81** (1998) 1183.

[21] S. Nemoto *et al.*, Phys. Rev. C **58** (1998) 2599.

[22] J. W. Holt, N. Kaiser, and W. Weise, Phys. Rev. C **79** (2009) 054331.

[23] D. R. Entem and R. Machleidt, *Phys. Rev. C* **66** (2002) 014002.

[24] N. Kaiser, Phys. Rev. C **64** (2001) 057001.

[25] N. Kaiser, Phys. Rev. C **65** (2002) 017001.

[26] D. R. Entem and R. Machleidt, *Phys. Rev. C* **68** (2003) 041001(R).

[27] R. Machleidt, Phys. Rev. C **63** (2001) 024001.

[28] V. G. J. Stoks, R. A. M. Klomp, C. P. F. Terheggen, and J. J. de Swart, Phys. Rev. C **49** (1994) 2950.

[29] R. B. Wiringa, V. G. J. Stoks, and R. Schiavilla, Phys. Rev. C **51** (1995) 38.

[30] E. Epelbaum, W. Glöckle, and U.-G. Meissner, Nucl. Phys. **A671** (2000) 295.

[31] S. Fritsch, N. Kaiser, and W. Weise, Nucl. Phys. **A750** (2005) 259.

[32] E. Epelbaum, *Prog. Part. Nucl. Phys.* **57** (2006) 654.

[33] J. Fujita and H. Miyazawa, *Prog. Theor. Phys.* **17** (1957) 360, 366.

[34] E. Epelbaum, A. Nogga, W. Glöckle, H. Kamada, U.-G. Meissner, and H. Witala, Phys. Rev. C **66** (2002) 064001.

[35] A. Nogga, P. Navratil, B. R. Barrett, and J. P. Vary, Phys. Rev. C **73** (2006) 064002.

[36] S. K. Bogner, T. T. S. Kuo, L. Coraggio, A. Covello, and N. Itaco, *Phys. Rev. C* **65** (2002) 051301(R).

[37] S. K. Bogner, T. T. S. Kuo, and A. Schwenk, *Phys. Rep.***386** (2003) 1.

[38] A. Nogga, S. K. Bogner, and A. Schwenk, *Phys. Rev. C* **70** (2004) 061002(R).

[39] S. K. Bogner, R. J. Furnstahl, and R. J. Perry, Phys. Rev. C **75** (2007) 061001(R).

[40] H. Feldmeier, T. Neff, R. Roth, and J. Schnack, Nucl. Phys. **A632** (1998) 61.

[41] T. Neff and H. Feldmeier, Nucl. Phys. **A713** (2003) 311.

[42] N. Kaiser, R. Brockmann, and W. Weise, *Nucl. Phys.* **A625** (1997) 758.

[43] K. Erkelenz, R. Alzetta, and K. Holinde, Nucl. Phys. **A176** (1971) 413.

[44] In order to facilitate the computation of symmetry factors and spin and isospin traces, we have modeled (for that purpose) the three-nucleon contact-interaction by heavy isoscalar boson exchanges.